

# A General Scheme for Suppression of ABX Strong Coupling Signals in Heteronuclear Scalar and Dipolar Correlation Experiments

Katalin E. Kövér\* and Gyula Batta†

\*Department of Organic Chemistry, L. Kossuth University, P.O. Box 20, H-4010 Debrecen, Hungary; and †Research Group For Antibiotics, Hungarian Academy of Sciences, L. Kossuth University, P.O. Box 70, H-4010 Debrecen, Hungary

Received October 6, 1998; revised December 15, 1998

**Enhanced versions of heteronuclear chemical shift correlation experiments which yield high-quality spectra with efficient suppression of extra peaks arising from strong coupling effects are proposed. The enhanced pulse sequences feature properly designed filtering schemes inserted during preparation, or prior to acquisition, or at both places depending on the particular experiment. These modifications extend the applicability of existing methods, since they exclude misinterpretation of spurious peaks and allow unambiguous assignment of the desired correlations. The general applicability of the filtering method is noteworthy; both scalar- and dipolar-correlated experiments with both X and <sup>1</sup>H detection using phase cycling or gradient pulses for coherence selection can be freed of strong coupling artifacts.** © 1999 Academic Press

**Key Words:** strong coupling; suppression of artifacts; X<sup>1</sup>H filtering; heteronuclear correlations.

## INTRODUCTION

Heteronuclear chemical shift correlation spectroscopy with both heteronucleus (1–3) and <sup>1</sup>H detection (4–6) has become an invaluable tool in the study of complex organic molecules. The cross-peaks appearing in the heteronuclear scalar-correlated spectra normally allow unambiguous assignment of the corresponding resonances of spin pairs. In the heteronuclear dipolar-correlated (HOESY) (7–10) experiment the cross-peaks arising from the cross-relaxation effect, in addition to corroborating the spectral assignment, provide structural information related to the spatial proximity of the relevant nuclei.

However, as was demonstrated earlier (11–24), strong coupling effects in an H<sub>(A)</sub>–<sup>13</sup>C<sub>(X)</sub>/<sup>12</sup>C–H<sub>(B)</sub> spin system where  $J_{AB} \neq 0$  and  $\Delta\nu_{AB} \approx \frac{1}{2} J_{AX}$  can result in the appearance of extra peaks which correlate the distant proton H<sub>(B)</sub> with <sup>13</sup>C<sub>(X)</sub> in addition to the direct correlation of H<sub>(A)</sub>–<sup>13</sup>C<sub>(X)</sub>. This leads to ambiguities in the spectral analysis of both scalar- (11–17) and dipolar- (20–25) correlated spectra generated via the conventional pulse sequences. Theoretical analysis of strong coupling effects in 2D experiments reported earlier (13, 18, 19) shows that the intensity of these artifacts can reach 30–50% of the

main peak in the case of heteronuclear scalar correlation. The situation can be even worse in heteronuclear dipolar-correlated experiments where the extra peaks are further enhanced during the mixing period by magnetization transfer via the zero-quantum coherences (21). These facts emphasize the need for a general method for suppression of strong coupling artifacts. Here we demonstrate that by using properly designed filters, undesired signals of strong coupling origin can be suppressed. We believe that the efficiency and general applicability of the proposed methods circumvent the limitations of the earlier ones. The pulse sequences extended with appropriate filtering schemes displayed in Fig. 1 are illustrated using simple disaccharides ( $\alpha,\alpha$ -D-trehalose (Scheme 1) and D-sucrose), presenting classic examples of strongly coupled spin systems.

## RESULTS AND DISCUSSION

### Heteronuclear Scalar Correlation

Several attempts to suppress the spurious peaks arising from strong coupling effects have been published in the literature. In the X-detected heteronuclear correlation experiment, application of broadband X decoupling during the  $t_1$  evolution interval (11, 12), incorporation of a BIRD pulse in the middle of  $t_1$  (14, 15), or generation of heteronuclear multiple-quantum evolution (16–18) has been previously proposed. Here we propose an alternative method that is applicable in both X- and <sup>1</sup>H-detected experiments using either phase cycling or pulsed field gradient for coherence selection.

The enhanced versions of the scalar-correlated experiments (Figs. 1a and 1b) correspond to a simple modification of the original sequences incorporating an X filter (26–28) during preparation or prior to acquisition depending on the particular mode (X or <sup>1</sup>H) of detection. Insertion of the X filter in the preparation part of the gradient-enhanced X-detected experiment (Fig. 1a) gives rise to different phase modulation of the <sup>1</sup>H–(<sup>12</sup>C) and <sup>1</sup>H–(<sup>13</sup>C) proton magnetization due to the heteronuclear one-bond coupling evolution during the filter of (1/J(XH)). In practice, two experiments are performed, one

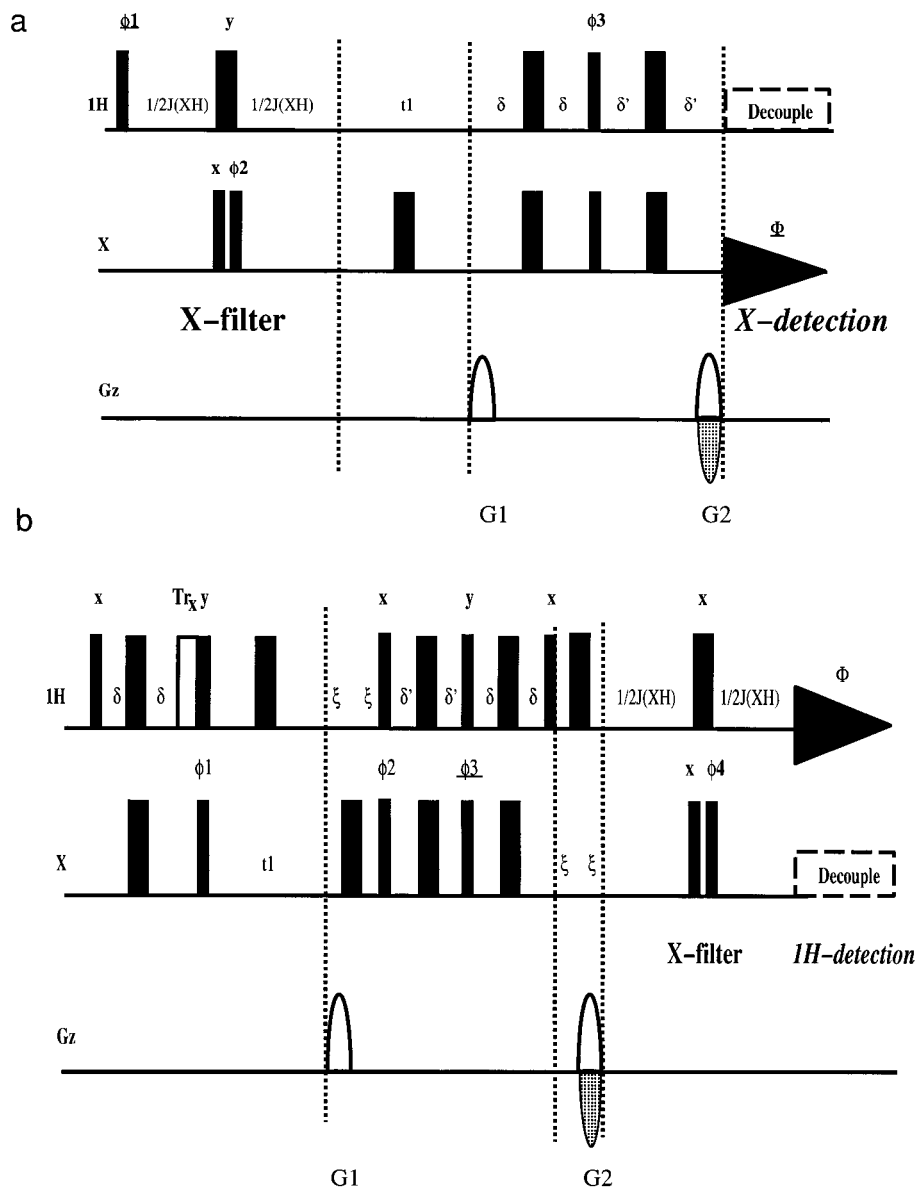


**FIG. 1.** The summary of the enhanced pulse sequences proposed in this study. Thin and thick bars represent  $90^\circ$  and  $180^\circ$  pulses, respectively. Phases are  $x$  if not indicated otherwise. (a) Gradient-enhanced X-detected  $^1\text{H}$ -X correlation experiment including X filter for suppression of strong coupling artifacts. Details of filtering are discussed in the text. Sine bell-shaped  $z$  gradient pulses of duration of 1 ms and  $G1:G2 = \gamma_X:\gamma_H$  were applied for echo-antiecho/TPPI gradient selection. The echo-antiecho signals were obtained by alternatively inverting the amplitude of G2 for consecutive FIDs, while the phases,  $\phi_1$  and  $\Phi$ , were inverted with each increment of  $t_1$ . A four-step phase cycle includes phase inversion of the first  $90^\circ$   $^1\text{H}$  pulse ( $\phi_1$ ) with simultaneous inversion of the receiver phase ( $\Phi$ ) in the first two transients. During the third and fourth transients the phase inversion of  $\phi_2$  followed by the receiver selects for the desired correlations, while those of strong coupling origin are efficiently suppressed.  $\phi_1 = x, -x$ ;  $\phi_2 = x, x, x, -x, -x, -x$ ;  $\Phi = x, -x, -x, x$ ;  $\delta = 1/(4^1J_{\text{XH}})$ ;  $\delta' = 1/(4^1J_{\text{XH}})$  or  $1/(6^1J_{\text{XH}})$  depending on the multiplicity selection for X. (b) Sensitivity- and gradient-enhanced HSQC experiment including X filter. A trim pulse ( $\text{Tr}_{xy}$ ) of 2–3 ms is included after the  $2\delta$  ( $\delta = 1/(4^1J_{\text{XH}})$ ) period to reduce  $^1\text{H}$ -( $^{13}\text{C}$ ) magnetization. Sine bell-shaped  $z$  gradient pulses of duration of 1 ms (where  $\zeta = 1.2$  ms includes a recovery delay of 0.2 ms) and  $G1:G2 = \gamma_H:\gamma_X$  were applied for echo-antiecho coherence selection; the amplitude of G2 and the phase,  $\phi_3$ , are alternatively inverted for consecutive experiments.  $\phi_1 = x, -x$ ;  $\phi_2 = x, x, -x, -x$ ;  $\phi_3 = y, y, -y, -y$ ;  $\phi_4 = x, x, x, x, -x, -x, -x, -x$ ;  $\Phi = x, -x, -x, x, -x, x, x, -x$ . The phase inversion of  $\phi_4$  followed by the inversion of the receiver phase allows suppression of strong coupling artifacts, as discussed in the text. (c) HOESY experiment extended with the double filter. Due to the simultaneous phase inversion ( $\phi_2$ ) of the second  $90^\circ$  pulse within the filters, the signals arising from the dipolar interactions of the protonated and nonprotonated heteronuclei have the same phase properties, allowing their simultaneous detection with a constant receiver phase, while the strong coupling signals experiencing only a single phase inversion are eliminated.  $\phi_1 = x$  (and TPPI is applied for phase sensitive detection);  $\phi_2 = -x, -x, -x, -x, x, x, x, x$ ;  $\phi_3 = x, x, -x, -x$ ;  $\Phi = x, x, -x, -x, x, x, -x, -x$ . (d) Gradient-enhanced proton-detected HOESY extended with the double filter. Sine bell-shaped  $z$  gradient pulses of duration of 1 ms (where  $\zeta = 1.2$  ms includes a recovery delay of 0.2 ms) and  $G1:G2 = \gamma_H:\gamma_X$  were applied for echo-antiecho/TPPI gradient selection; the amplitude of G2 is alternatively inverted for consecutive FIDs, as well as the phases,  $\phi_1$  and  $\Phi$ , are inverted with each  $t_1$  increment. Broadband proton decoupling (WALTZ using  $^1\text{H}$   $90^\circ$  of 250  $\mu\text{s}$ ) was applied during the relaxation delay and  $t_1$  evolution period.  $\phi_1 = x, -x$ ;  $\phi_2 = -x, -x, -x, -x, x, x, x, x$ ;  $\phi_3 = x, x, -x, -x$ ;  $\Phi = x, -x, -x, x, x, -x, -x, x$ .

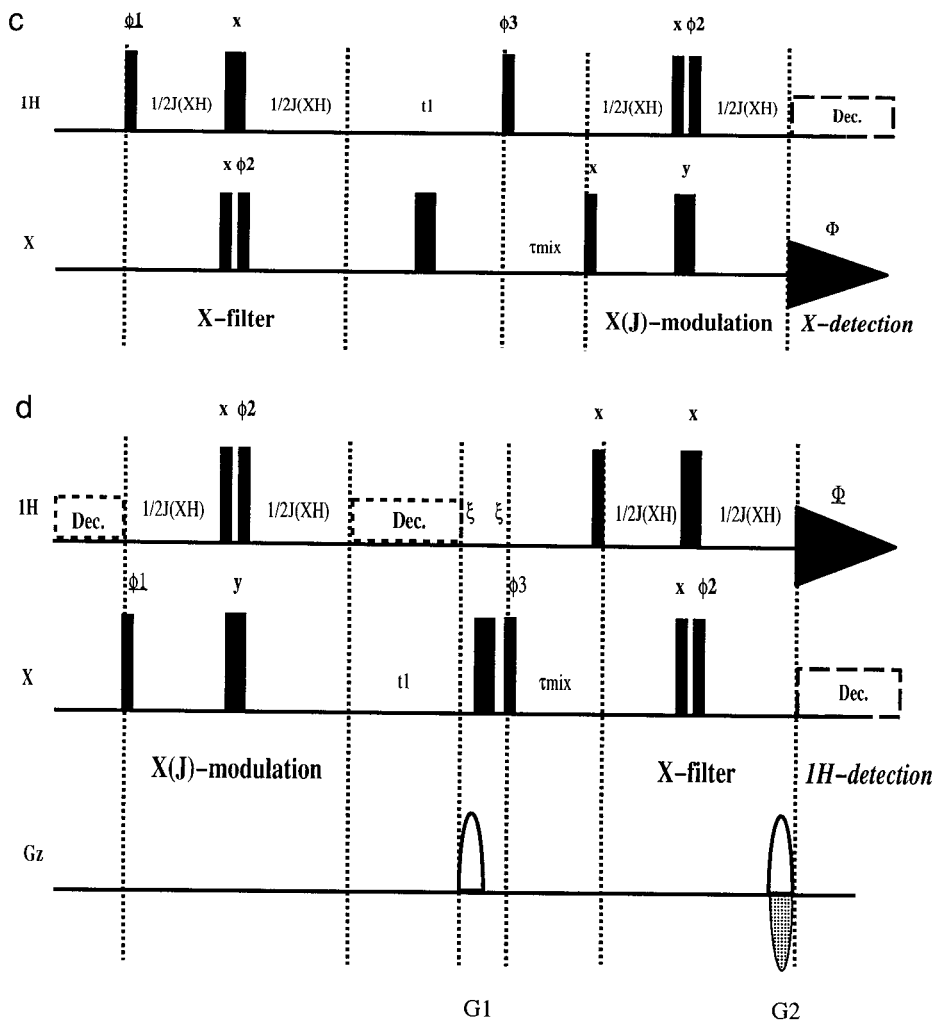
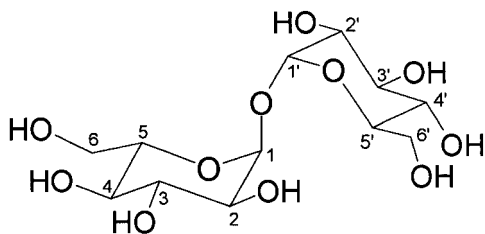


FIG. 1—Continued

with the same phase for the two  $90^\circ$   $X$  pulses to produce a  $180^\circ$  pulse on the  $X$  spin, and one with a phase difference of  $180^\circ$  for the two  $90^\circ$  pulses producing an effective  $0^\circ$  pulse. With appropriate phase cycling, i.e., following the phase inversion of the direct correlations by the receiver, these coherences are selected and observed. The spurious ones ( $^1\text{H}$ - $^{12}\text{C}$ - $^{13}\text{C}$ ) arising from strong coupling are eliminated by subtraction after every

two transients. The same applies for the enhanced  $^1\text{H}$ -detected correlation experiment (Fig. 1b), except that in this case, the purging filter is applied prior to the acquisition period. The remote protons ( $^1\text{H}$ - $^{12}\text{C}$ - $^{13}\text{C}$ ) remain unaffected due to the filter while the  $^{13}\text{C}$ -bound direct protons are phase encoded due to the evolution of heteronuclear one-bond coupling. Again, the different phase modulation of the magnetization of remote and direct protons allows their efficient separation. Figure 1b displays only the sensitivity- and gradient-enhanced (29–31) variants of the experiment; however, the filtering works with any other version of the correlation experiment. The applicability of the above sequences for generating artifact-free spectra is demonstrated by the spectra of D-trehalose as shown in Figs. 2 and 3, using  $X$  and  $^1\text{H}$  detection, respectively. In the spectra recorded by the original sequences (3, 29) (Figs. 2a and 3a), the extra peaks, H3/C2 and H2/C3, arising from strong coupling effects are indicated by asterisks. From the partial



SCHEME 1

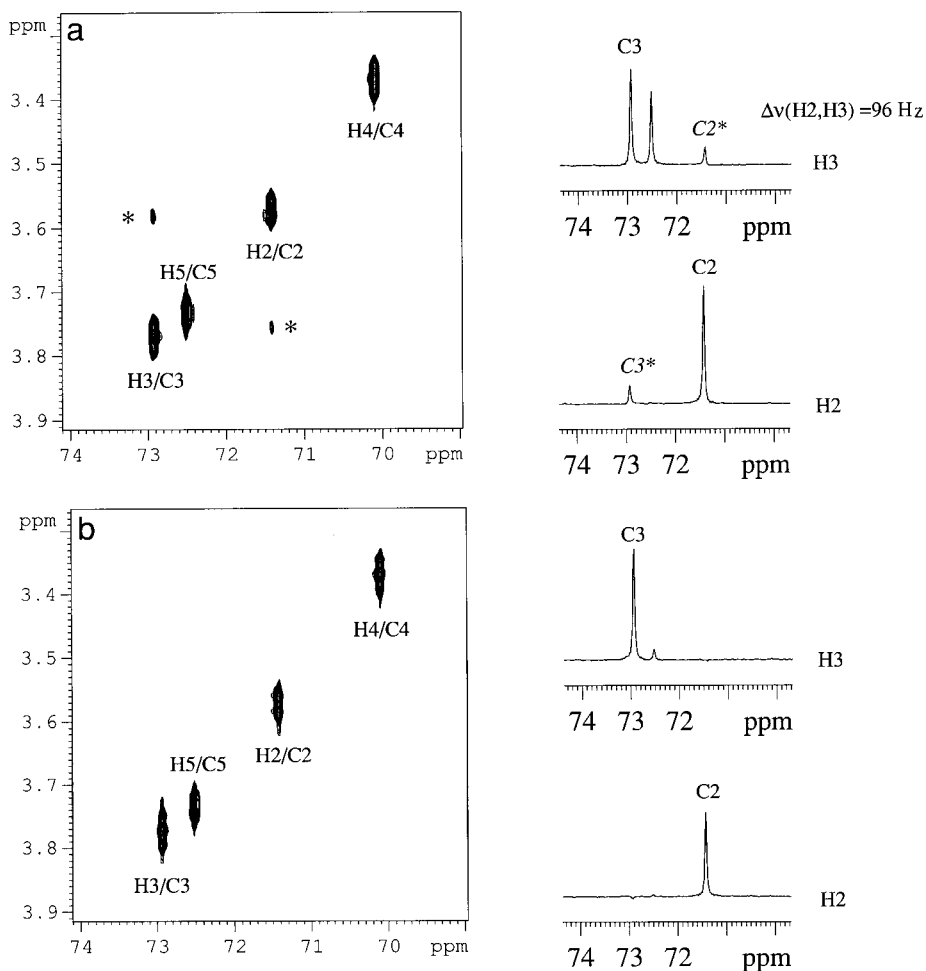


**FIG. 2.** Partial 2D  $^1\text{H}/^{13}\text{C}$  correlation spectra and corresponding selected  $F_2$  traces of  $\alpha,\alpha$ -D-trehalose (1.7 M in  $\text{D}_2\text{O}$ ). (a) Spectrum obtained with the conventional pulse sequence (3), but using echo-antiecho/TPPI coherence selection for phase-sensitive detection. Strong coupling artifacts are indicated by asterisks. (b) Spectrum recorded with the enhanced pulse sequence of Fig. 1a under the same experimental conditions. Spectral widths were 5040 Hz for  $^{13}\text{C}$  and 1250 Hz for  $^1\text{H}$ . Eight transients were accumulated for each of the 256 increments with a relaxation delay of 2 s;  $\delta$  ( $\delta'$ ) delay was set to 1.65 ms. The filter delay ( $1/(2^1J_{\text{XH}})$ ) was 3.3 ms; 2048 complex data points were acquired in  $F_2$ . Zero-filling in  $F_1$ , an exponential window function with line broadening of 3 Hz in  $F_2$ , and a cosine function in  $F_1$  were applied prior to Fourier transformation. The echo-antiecho protocol of standard Bruker software was applied for transformation. The spectra have been plotted at the same threshold.

contour plots and selected cross-sections of Figs. 2b and 3b, it is evident that the spurious peaks which appeared in the spectra acquired with the conventional pulse sequences disappeared from the maps recorded by the enhanced sequences of Figs. 1a and 1b. Therefore, we believe that for routine acquisition of artifact-free scalar-correlated spectra, the sequences of Figs. 1a and 1b are possibly the method of choice as long as the inherent sensitivity loss due to mistuning of the filter delay and  $T_2$  relaxation during the extended experiments is acceptable. This way signals due to strong couplings cannot be attributed to impurities of the compound. It should be noted that strong coupling artifacts could sometimes be put to good use by correlating vicinal connectivity.

### Heteronuclear Dipolar Correlation

Both theoretical (21) and experimental (20, 22, 23) analyses of HOESY experiments demonstrate that the intensity of the strong coupling artifact can even surpass that of the direct peak in unfortunate cases. Thus misinterpretation of these intense artifacts as real dipolar correlation peaks is a potential danger and can lead to false structural conclusions.

In earlier proposed modifications of the HOESY experiment to obtain artifact-free spectra, the application of a BIRD pulse (10, 20, 22) or  $MQ$  evolution (23) during  $t_1$  leads to undesired elimination of the dipolar correlations corresponding to the nonprotonated heteronuclei. This is hardly an acceptable toll

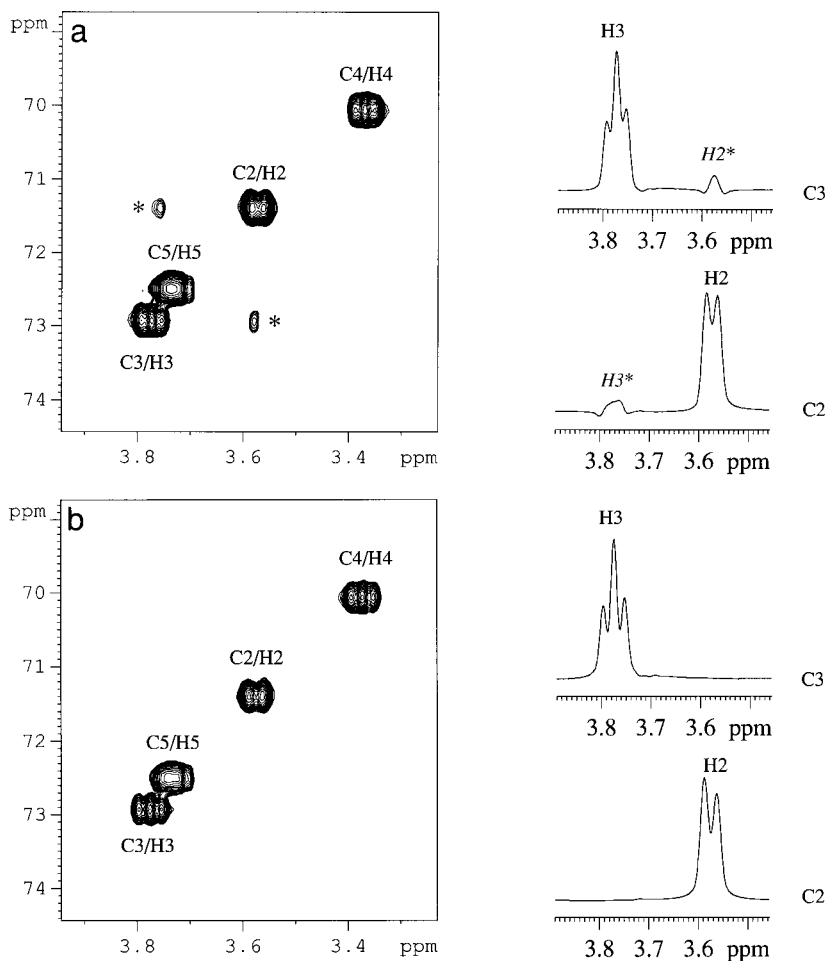


**FIG. 3.** Partial 2D HSQC spectra and corresponding selected  $F_2$  traces of  $\alpha,\alpha$ -D-trehalose (1.7 M in  $D_2O$ ). (a) Spectrum obtained with the conventional sensitivity- and gradient-enhanced pulse sequence (29). Strong coupling artifacts are indicated by asterisks. (b) Spectrum recorded with the enhanced pulse sequence of Fig. 1b under the same experimental conditions. Eight transients were accumulated for each of the 256 increments with a relaxation delay of 2 s;  $\delta$  ( $\delta'$ ) delay was set to 1.65 ms. The filter delay ( $1/(2^1J_{CH})$ ) was 3.3 ms; 512 complex data points were acquired in  $F_2$ . Zero-filling in both  $F_2$  and  $F_1$ , a squared cosine window function in  $F_2$ , and a cosine function in  $F_1$  were applied prior to Fourier transformation.

paid for artifact-free spectra, since invaluable structural information is completely lost. Another simple modification of the original HOESY experiment involves the use of simultaneous  $^1H$   $60^\circ$  and  $^{13}C$   $180^\circ$  pulses in the middle of the mixing period (20). A theoretical analysis (21) of the modified experiment shows that although the proposed sequence is effective in eliminating the strong coupling artifacts, it also leads to undesired (50–60%) attenuation of the dipolar correlations. It is also noteworthy that a modification of this type works only in the fast motion molecular regime. These limitations of the earlier methods emphasize the paramount need for a generally applicable approach free of the handicaps mentioned above.

Here we demonstrate that by inserting two filtering blocks, one in the preparation period and another prior to the acquisition in the original experiment, we can eliminate the undesired extra peaks of strong coupling origin, whereas the dipolar correlations of both protonated and nonprotonated heteronuclei are retained.

In the  $X$ -detected version of the HOESY experiment (7–10, 32) (Fig. 1c) an  $X$  filter is incorporated during preparation and an extra  $X(J)$  modulation (which can be also referred as a  $^1H$  filter) of  $X$  magnetization is allowed before acquisition. The first filter introduces a phase inversion of the  $^{13}C$ -bonded proton magnetization, while protons attached to  $^{12}C$  are not affected, as was discussed above in the case of scalar correlation. The  $J$ -modulation interval ( $^1H$  filter) applied before detection leads to an additional inversion of the signals of the protonated heteronuclei, leading to a different phase modulation of the desired and undesired correlations. As a final outcome of the sequence, the dipolar correlations of the protonated heteronuclei, due to the double phase inversion introduced by the filters, have the same phase properties as those of the nonprotonated heteronuclei, while the signals of strong coupling origin experience only a single phase inversion allowing their elimination by appropriate phase cycling. Note

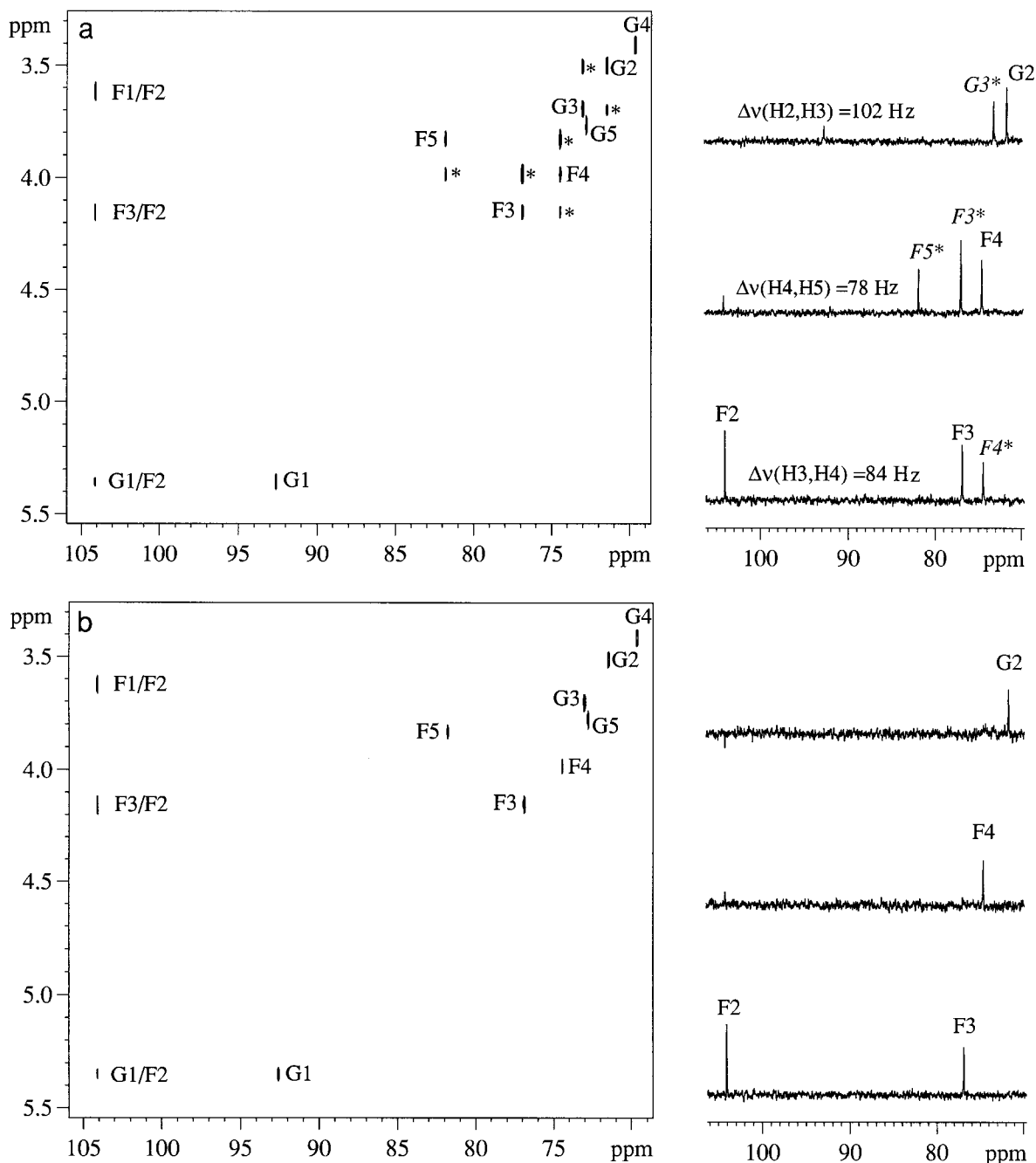


**FIG. 4.** Phase-sensitive 2D HOESY spectra and corresponding selected  $F_2$  traces of D-sucrose (1.7 M in  $D_2O$ ). (a) Spectrum obtained with the conventional pulse sequence (7), using TPPI for phase-sensitive detection. Strong coupling artifacts are indicated by asterisks. (b) Spectrum recorded with the enhanced pulse sequence of Fig. 1c under the same experimental conditions. Spectral widths were 7546 Hz for  $^{13}C$  and 1313 Hz for  $^1H$ . Ninety-six transients were accumulated for each of the 96 increments with a relaxation delay of 2 s. A mixing time ( $\tau_{mix}$ ) of 1.5 s was allowed for cross-relaxation. Filter delay ( $1/(2^1J_{XH})$ ) was 3.3 ms; 2048 complex data points were acquired in  $F_2$ . Experiment time was ca. 9 h. Zero-filling in  $F_1$  to 256, an exponential window function with line broadening of 3 Hz in  $F_2$ , and a squared cosine function in  $F_1$  were applied prior to Fourier transformation.

that the above modification of the original HOESY experiment can also be applied to the gradient-enhanced X-detected HOESY variant.

In the gradient-enhanced, proton-detected heteronuclear

NOESY (33) experiment (Fig. 1d), the first filtering block ( $^1H$  filter) inserted in the preparation period introduces a phase inversion of the magnetization of protonated heteronuclei due to the heteronuclear one-bond coupling evolution during the

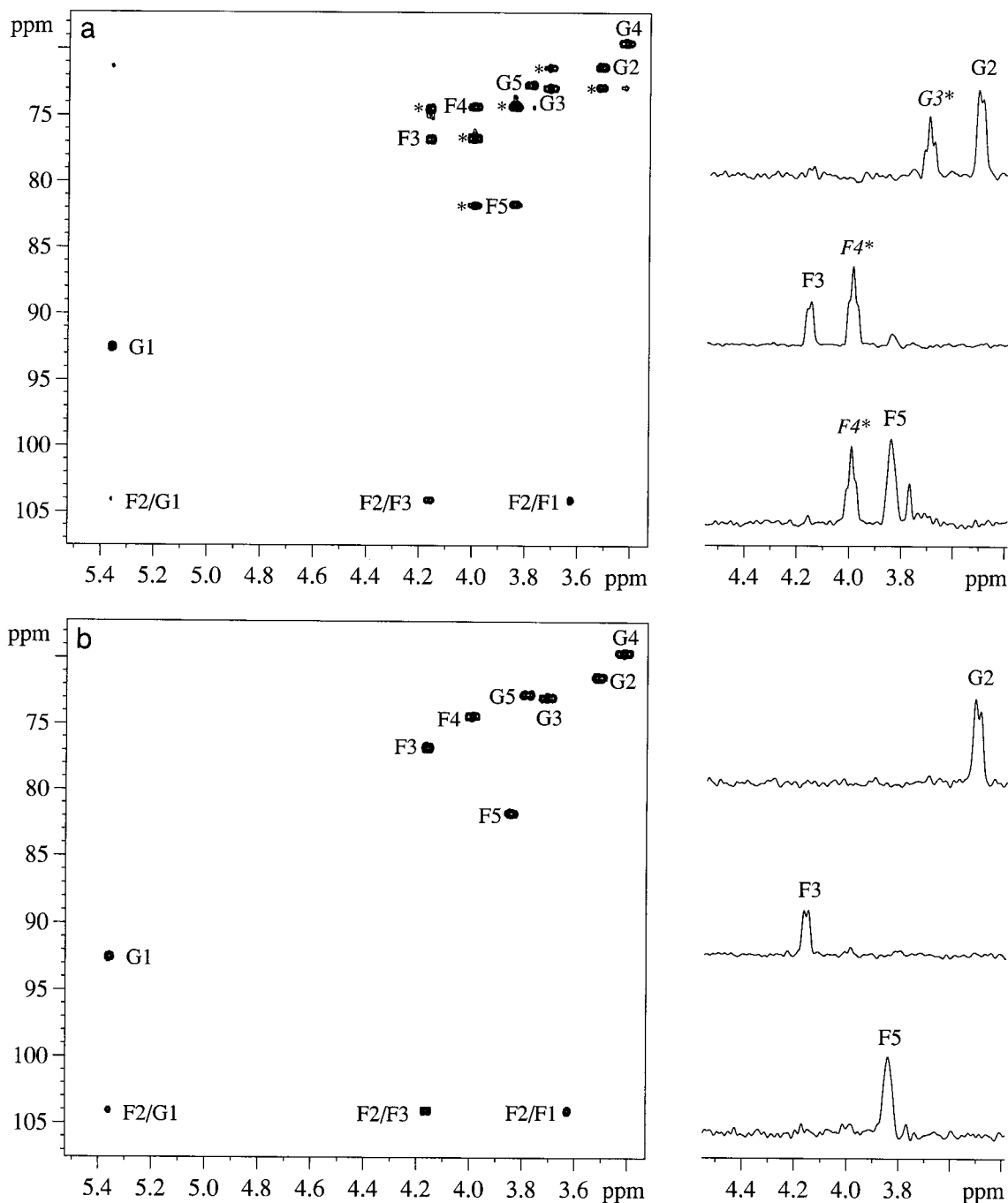


**FIG. 5.** Phase-sensitive, proton-detected 2D HOESY spectra and corresponding selected  $F_2$  traces of D-sucrose (1.7 M in  $D_2O$ ). (a) Spectrum obtained with the conventional pulse sequence (33), using echo-antiecho/TPPI gradient selection for phase-sensitive detection. Strong coupling signals are indicated by asterisks. (b) Spectrum recorded with the enhanced pulse sequence of Fig. 1d under the same experimental conditions. Sixteen transients were accumulated for each of the 256 increments with a relaxation delay of 2 s. A mixing time ( $\tau_{\text{mix}}$ ) of 1.5 s was allowed for cross-relaxation. Filter delay ( $1/(2^1J_{\text{XH}})$ ) was 3.3 ms; 512 complex data points were acquired in  $F_2$ . Experiment time was ca. 3 h. Zero-filling and squared cosine window functions were applied in both  $F_1$  and  $F_2$  prior to Fourier transformation. The echo-antiecho protocol of standard Bruker software was applied for transformation.

filter. The  $X$  filter inserted before acquisition generates an additional phase inversion of the respective correlations, allowing simultaneous detection of signals with identical phase

properties, i.e., those originating from the dipolar correlations of the protonated and nonprotonated heteronuclei. Again, the signals arising from strong coupling effects experience only

one phase inversion, which allows their efficient suppression by concerted phase cycling of the receiver. In this case, during the relaxation delay, broadband proton decoupling is applied to enhance the initial  $X$  magnetization by nonselective heteronuclear NOE depending on the efficiency of the dipolar cross-relaxation and the motional regime. The pulsed field gradients applied for echo-antiecho coherence selection provide excellent suppression of background ( $^1\text{H}$ - $^{12}\text{C}$ ) proton magnetization, leading to high-quality spectra. To reduce the diffusion-related sensitivity losses during the intervals between the gradients, the strength of the gradient pulse is kept at minimum, still sufficient for coherence selection. Due to the exceptional quality of HOESY spectra and the efficient suppression of strong coupling artifacts, unambiguous observation of small heteronuclear NOE enhancements becomes feasible. The relative sensitivity of  $X$ - and  $^1\text{H}$ -detected HOESY experiments depends on several factors (e.g., the relative size of NOE enhancements, the intrinsic relaxation rates of relevant spins, and the repetition rate) which are difficult to consider in general; however, our experimental results (see below) demonstrate the superior sensitivity of  $^1\text{H}$  detection.

The utility of the sequences in Figs. 1c and 1d for generating artifact-free HOESY spectra is demonstrated by the spectra of  $\text{D}$ -sucrose displayed in Figs. 4 and 5, recorded using  $X$  and  $^1\text{H}$  detection, respectively. Both the contour plots and the selected F2 traces taken through the 2D spectra illustrate the quality of artifact suppression achieved by the proposed methods in comparison with the original experiments. The traces in Figs. 4a and 5a are taken from the spectra acquired by the original pulse sequences (7–10, 33) and serve as reference, while the traces in Figs. 4b and 5b correspond to the filter-enhanced spectra acquired using the pulse sequence of Figs. 1c and 1d, respectively. Note that in the conventional HOESY under the applied experimental conditions the intensities of some artifacts (e.g., H4/C3 of fructose ring, marked by F3\* and F4\* in the middle trace of Figs. 4a and 5a, respectively) can even surpass those of the direct peaks. In general, the intensities of the extra peaks resulting from strong coupling effects (marked by asterisks in the spectra) are comparable to those of the direct dipolar correlations. The lack of these intense, easily misinterpretable signals in the filtered spectra clearly demonstrates the efficiency of the proposed filtering scheme. Moreover, it is important to emphasize again that the long-range dipolar correlations of the quaternary carbons, namely the F2 of  $\text{D}$ -sucrose in our case, survive the double filters and show the expected intra- and interring heteronuclear NOE correlations (marked by F1/F2, F3/F2, and G1/F2 in the contour plots of Figs. 4 and 5). It should be noted, however, that the proposed double-filtering approach is not applicable for detection of NOE contacts of protonated  $X$  nuclei with protons other than the directly bonded one. This is because dipolar correlation of that kind experiences the same phase modulation as the signals arising from strong coupling effects. In this case the conventional HOESY

experiment can be applied provided that strong coupling is not present in the  $X$  isotopomer spin system. Absence of strong coupling can be justified by checking the relevant spectral parameters (chemical shifts and scalar couplings). However, when detection of intra- or intermolecular heteronuclear NOE contacts between identical sites (i.e., remote proton and proton bound to  $X$  have the same chemical shift) is desired, the  $J$ -separated HOESY (34, 35) experiment can be the method of choice, as was nicely demonstrated by Mutzenhardt *et al.* (35).

## CONCLUSIONS

In summary, we propose enhanced versions of the heteronuclear scalar- and dipolar-correlated experiments that incorporate efficient filtering blocks for suppression of strong coupling artifacts. The proposed pulse sequences yield high-quality, artifact-free spectra and allow unambiguous assignment of both scalar and dipolar correlations. The general applicability of the filtering approach has been demonstrated; both  $X$ - and  $^1\text{H}$ -detected, as well as gradient-enhanced and phase-cycled variants of heteronuclear correlated experiments, have been tested. Finally, it is also noteworthy that the proposed filtering scheme is effective regardless of the motional properties of the molecules and leads to only slight sensitivity loss due to  $T_2$  relaxation and/or mistuning of the filter delay. We believe that the enhanced pulse sequences can be recommended as generally applicable methods for routine acquisition of spectra free from ABX strong coupling artifacts with potential applications for macromolecules, e.g., polymers and polysaccharides.

## EXPERIMENTAL

All experiments were performed on a Bruker Avance DRX-500 spectrometer, operating at 11.8 T, equipped with a 5-mm triple-resonance probe ( $^1\text{H}/^{13}\text{C}/^{15}\text{N}$ ) and actively shielded  $z$  gradient coil.  $^1\text{H}$  and  $^{13}\text{C}$   $90^\circ$  pulses were 11 and 13  $\mu\text{s}$ , respectively. In the  $X$ -detected experiments for proton decoupling during acquisition, the WALTZ scheme was applied at reduced power ( $90^\circ$   $^1\text{H}$  pulse of 100  $\mu\text{s}$ ). In the proton-detected experiments, the GARP sequence with a  $90^\circ$   $X$  pulse of 75  $\mu\text{s}$  was used for decoupling. The maximum gradient available was 50 G/cm. Sine bell-shaped gradient pulses with amplitudes of 40 G/cm (for  $^{13}\text{C}$ ) and 10 G/cm (for  $^1\text{H}$ ) were applied for coherence selection. All other experimental parameters are given in the figure legends.

## ACKNOWLEDGMENTS

K.E.K. and Gy.B. thank the National Research Foundation for financial support (OTKA T 014982 to K.E.K. and Gy.B.; OTKA D 23749 to K.E.K.). OMF B Mec-93-0098, Phare-Accord H-9112-0198, and OTKA A084 supported the purchase of the spectrometer used in the study. Support for methodological development provided by FKFP 500/1997 and by the International



Center for Genetic Engineering and Biotechnology CRP/HUN97-01(t2) is gratefully acknowledged.

## REFERENCES

1. A. A. Maudsley, L. Müller, and R. R. Ernst, Cross-correlation of spin-decoupled NMR spectra by heteronuclear two-dimensional spectroscopy, *J. Magn. Reson.* **28**, 463–469 (1977).
2. R. Freeman and G. A. Morris, Experimental chemical shift correlation maps in nuclear magnetic resonance spectroscopy, *J. Chem. Soc. Chem. Commun.* 684–686 (1978).
3. A. Bax and G. A. Morris, An improved method for heteronuclear chemical shift correlation by two-dimensional NMR, *J. Magn. Reson.* **42**, 501–505 (1981).
4. L. Müller, Sensitivity enhanced detection of weak nuclei using heteronuclear multiple quantum coherence, *J. Am. Chem. Soc.* **101**, 4481–4484 (1979).
5. G. Bodenhausen and D. J. Ruben, Natural abundance nitrogen-15 NMR by enhanced heteronuclear spectroscopy, *Chem. Phys. Lett.* **69**, 185–189 (1980).
6. R. R. Ernst, G. Bodenhausen, and A. Wokaun, "Principles of Nuclear Magnetic Resonance in One and Two Dimensions," Clarendon, Oxford (1987).
7. P. Rinaldi, Heteronuclear 2D-NOE spectroscopy, *J. Am. Chem. Soc.* **105**, 5167–5168 (1983).
8. C. Yu and G. C. Levy, Solvent and intramolecular proton dipolar relaxation of the three phosphates of ATP: A heteronuclear 2D NOE study, *J. Am. Chem. Soc.* **105**, 6994–6996 (1983).
9. Yu and G. C. Levy, Two-dimensional heteronuclear NOE (HOESY) experiments: Investigations of dipolar interactions between heteronuclei and nearby protons, *J. Am. Chem. Soc.* **106**, 6533–6537 (1984).
10. K. E. Kövér and Gy. Batta, Theoretical and practical aspects of one- and two-dimensional heteronuclear Overhauser experiments and selective  $^{13}\text{C}$   $T_1$ -determinations of heteronuclear distances, *Prog. NMR Spectrosc.* **19**, 223–266 (1987).
11. P. H. Bolton, A modest improvement in proton-carbon-13 chemical shift correlation spectroscopy, *J. Magn. Reson.* **51**, 134–137 (1983).
12. G. A. Morris and K. I. Smith, "Virtual coupling" in heteronuclear chemical-shift correlation by two-dimensional NMR. A simple test, *J. Magn. Reson.* **65**, 506–509 (1985).
13. G. A. Morris and K. I. Smith, Analysis of "virtual one-bond coupling" effects in heteronuclear chemical shift correlation 2D NMR spectra, *Mol. Phys.* **61**, 467–483 (1987).
14. V. Rutar, T. C. Wong, and W. Guo, Manipulated heteronuclear two-dimensional NMR utilizing bilinear pulses in the presence of strong coupling, *J. Magn. Reson.* **64**, 8–19 (1985).
15. G. V. T. Swapna, R. Ramachandran, Narsimha Reddy, and A. C. Kunwar, Virtual coupling effects in heteronuclear chemical-shift correlation spectroscopy, *J. Magn. Reson.* **88**, 135–140 (1990).
16. K. E. Kövér and Gy. Batta, Amended heteronuclear correlations by multiple-quantum evolution. Sensitivity enhancement, *J. Magn. Reson.* **86**, 384–390 (1990).
17. Gy. Batta and K. E. Kövér, Heteronuclear correlations by multiple-quantum evolution. II. Proton-proton "decoupling" and multiplicity labeling in a constant-time experiment using carbon detection, *J. Magn. Reson.* **89**, 553–561 (1990).
18. K. E. Kövér, Z. Mádi, and Gy. Batta, Amended heteronuclear correlations by multiple-quantum evolution. Theoretical aspects of an ABX spin system, *Magn. Reson. Chem.* **29**, 619–624 (1991).
19. A. D. Bain, I. W. Burton, and W. F. Reynolds, Artifacts in two-dimensional NMR, *Prog. NMR Spectrosc.* **26**, 59–89 (1994).
20. K. E. Kövér and Gy. Batta, Strong coupling effects and their suppression in two-dimensional heteronuclear NOE experiments, *J. Magn. Reson.* **74**, 397–405 (1987).
21. D. R. Muhandiram and R. E. D. McClung, Theoretical examination of a modified HOESY experiment, *J. Magn. Reson.* **80**, 539–546 (1988).
22. N. Sambasiva Rao, G. V. T. Swapna, Natarjan Hari, and R. Ramachandran, Strong coupling effects in heteronuclear NOE spectroscopy with bilinear rotation decoupling, *J. Magn. Reson.* **88**, 364–368 (1990).
23. K. E. Kövér and Gy. Batta, Amended heteronuclear correlations by multiple-quantum evolution. III. Suppression of strong-coupling effects in 2D heteronuclear NOE experiments, *J. Magn. Reson.* **92**, 152–157 (1991).
24. G. Esposito, F. Fogolari, H. Molinari, M. Pegna, and L. Zetta, Proton strong coupling in heteronuclear systems. Theoretical and experimental evaluation in quantitative analysis of SQC NOESY spectra of biopolymers, *J. Magn. Reson. B* **101**, 240–247 (1993).
25. H. B. Seba and B. Ancian, 2D heteronuclear NOE study of intermolecular interactions between a solute carbon-13 nucleus and nearby solvent protons, *J. Magn. Reson.* **84**, 177–183 (1989).
26. D. Neuhaus, G. Wider, G. Wagner, and K. Wüthrich, X-relayed  $^1\text{H}$ - $^1\text{H}$  correlated spectroscopy, *J. Magn. Reson.* **57**, 164–168 (1984).
27. G. Otting, H. Senn, G. Wagner, and K. Wüthrich, Editing of 2D  $^1\text{H}$  NMR spectra using  $X$  half-filters. Combined use with residue-selective  $^{15}\text{N}$  labeling of proteins, *J. Magn. Reson.* **70**, 500–505 (1986).
28. G. Otting and K. Wüthrich, Heteronuclear filters in 2-dimensional ( $^1\text{H}$ ,  $^1\text{H}$ ) NMR spectroscopy—Combined use with isotope labeling for studies of macromolecular conformation and intermolecular interactions, *Q. Rev. Biophys.* **23**, 39–96 (1990).
29. L. E. Kay, P. Keifer, and T. Saarinen, Pure absorption gradient enhanced heteronuclear single quantum correlation spectroscopy with improved sensitivity, *J. Am. Chem. Soc.* **114**, 10663–10665 (1992).
30. G. Kontaxis, J. Stonehouse, E. D. Laue, and J. Keeler, The sensitivity of experiments which use gradient pulses for coherence-pathway selection, *J. Magn. Reson. A* **111**, 70–76 (1994).
31. D. R. Muhandiram and L. E. Kay, Gradient-enhanced triple-resonance 3-dimensional NMR experiments with improved sensitivity, *J. Magn. Reson. B* **103**, 203–216 (1994).
32. I. Furó, P. Mutzenhardt, and D. Canet, X-filtered HOESY experiment for detecting intermolecular contact between identical sites, *J. Am. Chem. Soc.* **117**, 10405–10406 (1995).
33. W. Bauer, Pulsed field gradient "inverse" HOESY applied to the isotope pairs  $^1\text{H}$ ,  $^{31}\text{P}$  and  $^1\text{H}$ ,  $^7\text{Li}$ , *Magn. Reson. Chem.* **34**, 532–537 (1996).
34. Gy. Batta and K. E. Kövér, New approaches to oligosaccharide sequencing and conformational distribution around the glycosidic bond. One- and two-dimensional  $^{13}\text{C}$ - $\{^1\text{H}\}$  NOE spectroscopy, *Magn. Reson. Chem.* **26**, 852–859 (1988).
35. P. Mutzenhardt, O. Walker, D. Canet, E. Haloui, and I. Furó, Anisotropy of molecular reorientation and geometrical information as determined from short and long range  $^{13}\text{C}$ - $^1\text{H}$  spin cross-relaxation rates, *Mol. Phys.* **94**, 565–569 (1998).